Turkish Journal of Electrical Engineering & Computer Sciences

http://journals.tubitak.gov.tr/elektrik/

Research Article

Turk J Elec Eng & Comp Sci
(2013) 21: 1376 – 1393

doi:10.3906/elk-1105-51

Optimal placement of PMUs using improved tabu search for complete observability and out-of-step prediction

Amany EL-ZONKOLY,* **Samah EL-SAFTY, Rana MAHER**
Department of Electrical and Control Engineering, College of Engineering and Technology,
Arab Academy for Science & Technology and Maritime Transport, Miami, Alexandria, Egypt

Received: 26.05.2011 • **Accepted:** 16.04.2012 • **Published Online:** 12.08.2013 • **Printed:** 06.09.2013

Abstract: This paper proposes an optimization method for the optimal placement of phasor measurement units (PMUs) for the complete observability of power systems. The proposed method is based on numerical observability and artificial intelligence. The artificial intelligence algorithm used is the improved tabu search (ITS) algorithm. The ITS is used to find the optimal placement for the PMU to keep the system completely observable. In addition, the paper describes a predictive out-of-step (OOS) algorithm based on the observation of the voltage phase difference between the substations. The proposed optimal placement of the PMUs and the OOS algorithm is tested using the IEEE 6-bus and IEEE 14-bus systems, and the Egyptian 500 kV network. The test systems are simulated using the power system computer aided design software program. The placement algorithm and the OOS prediction algorithm are carried out using MATLAB script programs.

Key words: Improved tabu search, observability, optimal placement

1. Introduction

Phasor measurement units (PMUs) are measuring devices synchronized via signals from global positioning system satellite transmission [1]. They are employed to measure the positive sequence of voltage and current phasors. By the synchronized sampling of microprocessor-based systems, phasor calculations can be placed on a common reference. The magnitudes and angles of these phasors comprise the state of the power system and are used in complete observability and transient stability analysis. The observability of a system can be assessed by considering the topology of the network and the types and locations of the measurements. Transient instability becomes more and more complicated as the power systems grow in scale and complexity. Out-of-step (OOS) studies become more essential to prevent large scale black-outs in power systems.

In recent years, there has been significant research activity on the problem of finding the minimum number of PMUs and their optimal locations. In [2], a bisecting search method was implemented to find the minimum number of PMUs to make the system observable. In [3], the authors used a simulated annealing technique to find the optimal PMU locations. In [4], a genetic algorithm (GA) was used to find the optimal PMU locations. The minimum number of PMUs needed to make the system observable was found using a bus-ranking methodology. In [5] and [6], the authors used integer programming to determine the minimum number of PMUs. The authors in [7] used the condition number of the normalized measurement matrix as a criterion for selecting candidate solutions, along with binary integer programming to select the PMU locations. In [8], the authors used the

*Correspondence: amanyelz@yahoo.com

tabu search (TS) algorithm to solve the optimal PMU placement problem. However, the number of PMUs was determined by trial and error and only their locations were determined using the TS algorithm. The authors in [9] proposed a particle swarm optimization (PSO)-based algorithm to find both the optimal number and locations for the PMUs to be placed, but their study did not cover cases such as the loss of the PMU or the loss of a branch of the network. In [10], an exhaustive search approach was proposed to determine the minimum number and optimal placement of the PMUs for state estimation, considering single branch outages only. In [11], the authors proposed a method to find the optimal conventional measurement set that is necessary for complete system numerical observability, considering a single measurement loss and single-branch outage contingency. Next, the positions of these measurements were rearranged by a heuristic algorithm in order to minimize the number of PMU placement sites. However, both the essential and the redundant conventional measurement sets were found by trial and error. The authors in [12] proposed a PMU placement algorithm that was based on a metaheuristic method. First, PMUs were placed at the most important network nodes, and then the iterated local search algorithm was used to minimize the number of PMUs needed to observe the network. The work limited the location and number of PMUs to be placed and did not consider the system during contingencies. In [13] and [14], the authors used binary PSO and modified binary PSO algorithms to find the optimal number and location of PMUs to maintain system observability. The proposed algorithms studied the system in the case of normal operation and in the case of the loss of a single branch or single measurement. However, the authors did not only depend on the PMU to maintain system observability, they also used the existing conventional measurements. In addition, the algorithm allowed the existence of solutions violating the observability constraint and did not neglect them from the beginning or during the search as in this paper. The optimal solution was then determined as the solution with minimum number of PMUs and the minimum number of unobservable buses. Integer programming was used in [15] to find the optimal location of the PMUs to make the system observable. However, the number of PMUs was preset to 10% of the bus number, chosen according to their priority index. To keep the system observable, the PMUs were fixed at these locations and the conventional supervisory control and data acquisition measurements were optimally located.

Various methods for OOS detection have been developed and are used in protection systems, such as tracking the trajectory of the impedance vector measured at the generator terminals [16], the rate of change of the apparent resistance augmentation [17], or the Lyapunov theory [18].

In this paper, an optimal search approach based on an improved TS (ITS) algorithm to determine the optimal number and locations of the PMUs for complete system observability is proposed first. The proposed algorithm is applied during normal system operation and also in 2 abnormal cases. It is applied in the case of the loss of a PMU and in the case of the loss of one of the network branches. The ITS is a combination of both the simple TS and the simple GA in a way to benefit from the advantages of both of the algorithms. The paper then introduces a predictive OOS algorithm based on measuring the phase difference among several generators from the voltage data collected at substation buses.

2. System observability analysis

The observability of a system can be assessed by considering the topology of the network and the types and locations of the measurements. The meter placement algorithm presented in this paper is based on a simple observability analysis method that was introduced earlier in [19] and [20]. This method will be briefly reviewed first.

2.1. Direct numerical method

Consider an N-bus system provided with m-measurements of voltage and current phasors contained in vector z. Vector z is linearly related to the N-dimensional state vector x containing N-nodal voltage phasors, resulting in n = 2N – 1 state variables [19]. This yields the linear model:

$$z = Hx + e, \tag{1}$$

where H is the $(m \times N)$ design matrix and e is an $(m\times\ 1)$ additive measurement error vector.

By splitting the vector z into the $(m_V\times\ 1)$ voltage and $(m_I\times\ 1)$ current subvectors, we have z_V and z_I, respectively. Moreover, by splitting the vector x into the $(N_M\times\ 1)$ measured and $(N_C\times\ 1)$ nonmeasured subvectors, V_M and V_C, respectively, relationship Eq. (1) becomes:

$$\begin{bmatrix} Z_V \\ Z_I \end{bmatrix} = \begin{bmatrix} 1 & 0 \\ Y_{IM} & Y_{IC} \end{bmatrix} \begin{bmatrix} V_M \\ V_C \end{bmatrix} + \begin{bmatrix} e_V \\ e_I \end{bmatrix}, \tag{2}$$

where 1 is the identity matrix and Y_{IM} and Y_{IC} are the submatrices whose entries are the series and shunt admittances of the network branches.

When the shunt elements are neglected, then the design matrix H reduces to:

$$H = \begin{bmatrix} 1 & 0 \\ M_{IB}Y_{BB}A_{MB}^T & M_{IB}Y_{BB}A_{CB}^T \end{bmatrix}, \tag{3}$$

where M_{IB} is the $(m_I\times$ b) measurement-to-branch incidence matrix associated with the current phasor measurements, Y_{BB} is the $(b \times b)$ diagonal matrix of the branch admittances, and A_{MB} and A_{CB} are the $(N_M \times b)$ measured and $(N_C \times b)$ calculated node-to-branch incidence submatrices, respectively.

2.2. The observability check

The decoupled gain matrix for the real power measurements can be formed as [20]:

$$G = H^T H \tag{4}$$

Note that since the slack bus is also included in the formulation, the rank of H (and G) will be at most (N – 1), even for a fully observable system. This leads to the triangular factorization of a singular and symmetric gain matrix.

The symmetric matrix G can be decomposed into its factors LDL^T, where the diagonal factor D may have one or more zeros on its diagonal. If it has more than one zero on its diagonal, then the system is unobservable.

3. TS algorithm

The TS algorithm is a powerful optimization procedure that has been successfully applied to a number of combinatorial optimization problems. It is an optimization method that was developed by Glover [21,22], specifically for combination optimization problems. It guides the search for the optimal solution, making use of memory systems that exploit its past history, and leads to the best solution. The fundamental concept of the simple TS involves individual, population, and generation. If v_k is the trial vector up to iteration k, Δv_k is a move, then $v_k + 1 = v_k + \Delta v_k$ is the trial vector at iteration k + 1. The set of all of the possible moves out of a current solution is called the set of candidate moves. One could operate with a subset of it.

3.1. Tabu restrictions

There are certain conditions imposed on the moves, which make some of them forbidden. These forbidden moves are known as tabu. A tabu list is formed to record these moves. A new trial vector satisfying the tabu restriction is classified as tabu. The dimension of the tabu list is called the *tabu list* size. Let v_{tabu} be any vector in the tabu list and let d_{tabu} be the tabu distance; for extending the simple TS to the real-valued optimization problem, a tabu restriction in the ITS can be expressed as:

$$|(v_k + \Delta v_k) - v_{tabu}| < d_{tabu}. \tag{5}$$

3.2. Aspiration criteria

Aspiration criteria can override tabu restrictions. That is, if a certain move is forbidden, the aspiration criteria, when satisfied, can reactivate this move. Let v_k^* be the best current solution, where the aspiration criteria can be expressed as:

$$|(v_k + \Delta v_k) - v_{tabu}| < d_{tabu}$$

with

$$\text{fitness } (v_k + \Delta v_k) < \text{ fitness } (v_k^*). \tag{6}$$

3.3. Development of the ITS algorithm

The 3 main parameters of the simple GA method are introduced to improve the simple TS algorithm. The 3 parameters are selection, mutation, and recombination. The ITS is developed as follows [23].

3.3.1. Initialization

Let $v_k = [b_1 \; ... \; b_d \; ... \; b_i \; ... \; b_N]$ be an initial vector representing the k*th* individual of a population, where N is the number of system buses. Let u be a uniformly distributed random number between 0 and 1, and PS is the population size, the initial vector v_k, k = 1... PS, is determined by setting its i*th* components b_i by:

$$b_i = \underline{b_i} + u * (\overline{b_i} - \underline{b_i}), \tag{7}$$

where $\overline{b_i}$ and $\underline{b_i}$ are the maximum and minimum values of the component b_i.

Calculate the fitness function of each individual, sort the fitness values in ascending order, and pick up the first τ_{max} individual to be placed in the initial tabu list, where τ_{max} is the maximum tabu list size.

3.3.2. Adaptive progressing scheme

The adaptive scheme used in this paper is defined by:

$$S(g+1) = \begin{cases} S(g) - S_\Delta; & C_{\min}(g) = C_{\min}(g-1) \\ S(g) & C_{\min}(g) < C_{\min}(g-1) \end{cases} \tag{8}$$

and

$$S(g+1) = S_{\min}; \text{ if } S(g) - S_\Delta < S_{\min}. \tag{9}$$

The adaptive scheme is used by setting S as equal to various parameters; α, β and τ in later sessions. C(g) is the fitness at generation number g, S_Δ is the step size related to the parameters under consideration, and S depends on the number of generations and the complexity of the system.

Let d_o be the initial value of tabu distance and let γ be a *drop factor*. For improving the ITS, an adaptive tabu distance is used in this paper by:

$$d_{tabu} = d_o * \gamma^g \tag{10}$$

A larger d_{tabu} can provide diversification in the beginning of the search and a smaller d_{tabu} provides intensification at the end of the search. Hence, the algorithm could intensify the search around an already elite small region without wasting invalid trips to improve performance. The power g is used to control the tabu distance, which is the generation number.

3.3.3. Mutation

Let $v_k = [b_1 \text{ ... } b_d \text{ ... } b_i \text{ ... } b_N]$ be the old kth vector and let $v'_k = [b'_1 \ldots b'_d \text{ ... } b'_i \text{ ... } b'_N]$ be the mutated kth vector, k = 1,... .,N_m. The ith element of v'_k is mutated by:

$$b'_i = b_i + N(\mu, \sigma^2), i \neq d, \tag{11}$$

where N_m is the number of mutated individuals that are randomly selected, and $N(\mu, \sigma^2)$ is a Gaussian random variable with mean of μ and variance of σ^2. In general, μ is set to 0 and σ^2 can be expressed by considering the fitness ratio as:

$$\sigma^2 = \frac{C_k}{C_{\max}}(\overline{b_i} - \underline{b_i})\beta, \tag{12}$$

where β is an adaptive mutation scale with S = β, $S_\Delta = \beta_\Delta$, and $S_{min} = \beta_{min}$. If b'_i exceeds its limit, it is set back to the limit.

3.3.4. Recombination

Recombination is a mechanism in which a new vector, v'_k, is generated using parameters from 2 randomly selected old vectors, v_{k1} and v_{k2}. It generates an individual with certain qualities inherited from both parents. The recombination function can be found by:

$$\begin{aligned} v'_k &= v_{k1} + u * (v_{k2} - v_{k1}) \\ &= [b'_1 ... b'_d ... b'_i ... b'_N], k = 1, ..., N_r \end{aligned} , \tag{13}$$

where N_r is the number of recombined individuals.

3.3.5. Determination of $\mathbf{N_m}$ and $\mathbf{N_r}$

N_m and N_r must satisfy:

$$N_m + N_r = PS \tag{14}$$

with

$$\begin{aligned} 0 \leq N_m \leq PS \\ 0 \leq N_r \leq PS \end{aligned}$$

N_m and N_r are both initialized to 1/2 PS. Mutation is a diversification strategy and recombination is an intensification strategy to reexplore previously visited attractive regions. With I as a designated intensification number, if the best solution C_{min}(g – 1) resulted from mutation and $C_{min}(g-1) > C_{min}(g)$, the number of mutated individuals in the next population will increase as:

$$\begin{array}{l} N_m(g+1) = N_m(g) + I \\ N_r(g+1) = PS - N_m(g+1) \end{array} . \tag{15}$$

Similarly, if the best solution C_{min}(g) resulted from recombination, we have:

$$\begin{array}{l} N_r(g+1) = N_r(g) + I \\ N_m(g+1) = PS - N_r(g+1) \end{array} . \tag{16}$$

On the other hand, for $C_{min}(g-1) = C_{min}(g)$, we have:

$$\begin{array}{l} N_m(g+1) = N_m(g) - I \text{ if } N_m(g) = N_m(g-1) + I \\ N_r(g+1) = N_r(g) - I \text{ if } N_r(g) = N_r(g-1) + I. \end{array} . \tag{17}$$

3.3.6. Evaluation and selection

Update the solution and assign a rank for the calculated fitness, RC$_k$, to each new vector, v'_k, k = 1, ..., PS. A best solution would gain the first number place, i.e. the highest rank

RC = 1. A combined population with 2 * PS individuals is formed with the old and new population. The concept of 'distance' was added to the fitness function to prevent the search from being trapped in a local minimum. A far away point needs a higher rank to be selected, even if the fitness is slightly worse. The fitness score of the k*th* individual is expressed as:

$$F_k = RC_k + \alpha * RD_k, k = 1, ..., 2 * PS, \tag{18}$$

where α is an adaptive decay scale with $S = \alpha$, $S_\Delta = \alpha_\Delta$, and S$_{min} = \alpha_{min}$; RD$_k$ is the rank of D$_k$, assigned to the k*th* individual (RD$_k$ = 1 for the largest D$_k$); TS the tabu list size; and D$_k$ is the sum of the distances from the individual to each solution vector in the tabu list and is given by:

$$D_k = \sum_{t=1}^{TS} |v_k - v_{tabu,t}|. \tag{19}$$

Individuals are ranked in a descending order according to their fitness scores. The first PS individuals are moved along with their fitness for the next generation. If the new population does not include the current best solution, the best solution must replace the last individual in the new population (Elitism).

3.3.7. Control of the tabu list

The tabu list is a finite length one-in one-or-more-out circular data structure that records the solutions just visited and all of the local optimal solutions visited so far. A new vector is placed on top of the list and the oldest vector is taken out of the list. An adaptive tabu list size τ(g) is given by setting S = τ, S$_\Delta$ = τ_Δ, and S$_{min}$ = τ_{min}, i.e. the tabu move is kept as tabu for a duration of τ moves. The choice of the tabu list size is critical. If the size is too small, cycling may occur in the searching process and the process often returns to the solution just visited. In contrast, if the size is too large, the required moves may become restricted and higher quality solutions cannot be explored. Empirically, a suitable tabu list size is in the range of 5 to 30 [23].

3.3.8. Stopping criterion

The stopping criterion may be a maximum number of generations to be reached, a specified best fitness to be reached, or a saturation of the value of the best fitness for a number of consecutive generations.

4. Optimal PMU placement algorithm

The proposed algorithm is applied to find the optimal measurement scheme such that the network is fully observable. That is why the observability check is carried out along with the tabu and aspiration checks for every individual of the population. The optimal scheme represents the essential measurement set. The fitness value of an individual is the cost of the PMUs placed.

The same procedure is repeated to find the locations of the extra PMUs needed to be placed in the case of the loss of a single PMU or the loss of a single branch of the branches of the system.

Such an application will lead to the required set of PMUs needed to keep the system fully observable under normal conditions and during the 2 contingencies of losing any PMU or any branch.

A MATLAB program is developed to fulfill the logical steps of the ITS algorithm, starting from the initialization of the first populations, and ending with determining the optimal placement of PMUs all over the power network.

The algorithm procedures of the ITS program can be summarized in the following steps:

1. Initiate a number of individuals that are constrained to be completely observable.
2. Calculate the costs (fitness function) of each individual and sort them in ascending order.
3. Pick up the first tabu list, with its tabu size set to maximum (τ_{max}), out of the sorted initial population.
4. Evaluate the constrained neighbors (new set of populations) through mutation and recombination.
5. Calculate the cost of each individual.
6. Check the tabu restriction and aspiration criteria.
7. Calculate the fitness and arrange all of the individuals in ascending order, and then pick up the new population.
8. Update all of the adaptive parameters, e.g., N_m, N_r, τ, β, and α.
9. Check the stopping criterion.

A flowchart for the developed ITS program is shown in Figure 1.

5. Optimal placement test results

5.1. IEEE 6-bus system

In the case of the IEEE 6-bus, the optimization algorithm yields the result that the system needs PMUs located at bus 1 and bus 5 for complete observability under normal operation. Moreover, the ITS yields the need of an extra PMU to be placed at bus 4 to guarantee the system observability in the case of the loss of any PMU or in the case of the loss of any branch of the system.

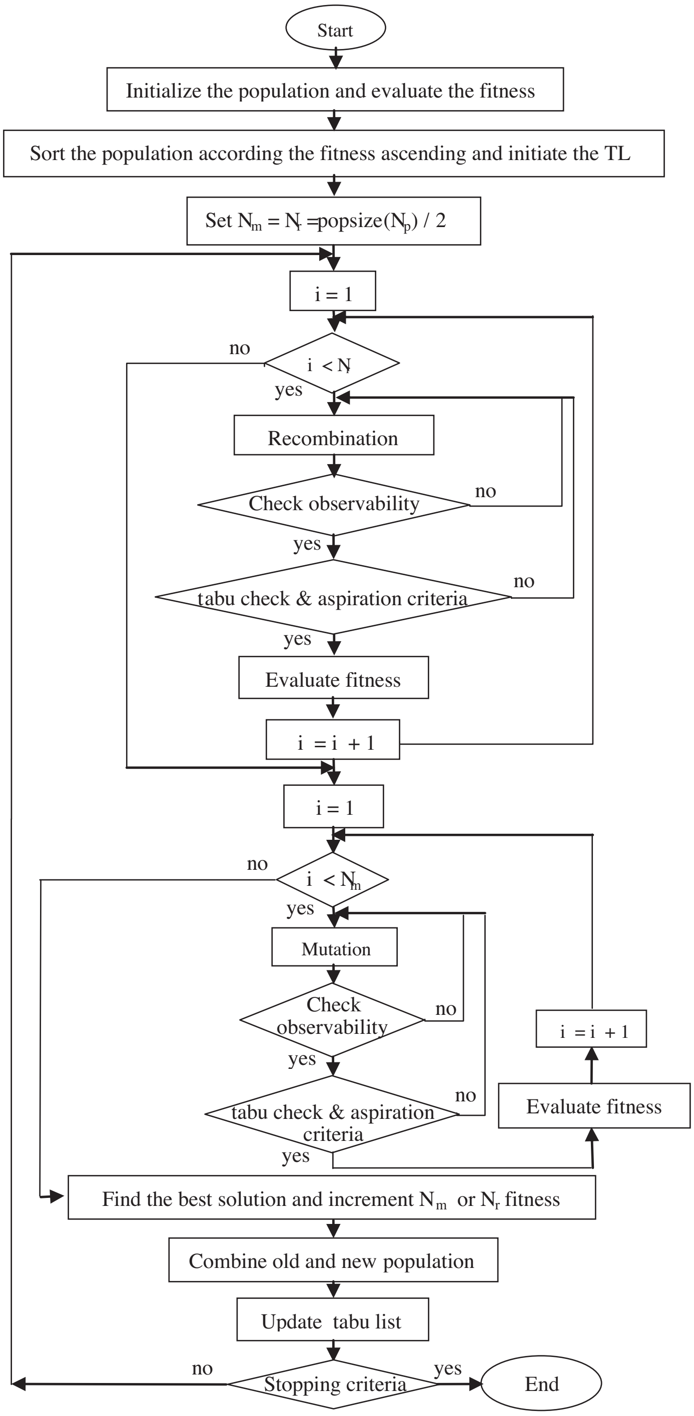

Figure 1. Flowchart for the developed ITS program.

5.2. IEEE 14-bus system

In case of the IEEE 14-bus, the optimization algorithm yields the result that the system needs PMUs located at buses 2, 6, and 9 for complete observability under normal operation, which is consistent with the results presented in [10].

The results of the ITS in the case of the loss of a single branch and in the case of the loss of a single PMU are represented in Tables 1 and 2, respectively. Table 1 shows only the branches that will cause the system to be unobservable when they are out of service. From Tables 1 and 2, it can be concluded that the extra PMUs that will keep the system observable in the case of the loss of any main PMU or the loss of a branch are to be placed at buses 1, 7, and 13.

Table 1. ITS results in the case of the loss of a single branch.

Branch out	Locations of the extra PMUs
1–2	1
2–3	1
6–11	1, 7
6–12	13
6–13	7, 13
7–9	13
9–10	1, 7
9–14	13

Table 2. The ITS results in the case of the loss of a single PMU.

Out PMU at bus	Locations of extra PMUs
2	1, 7
6	7, 13
9	7, 13

5.3. Egyptian 500 kV network

In the case of the Egyptian 500 kV network, the optimization algorithm yields the result that the system needs PMUs located at buses 3, 7, 8, and 12 for complete observability under normal operation. The results of the ITS in the case of the loss of a single branch and in the case of the loss of a single PMU are represented in Tables 3 and 4, respectively. From Tables 3 and 4, it can be concluded that the extra PMUs that will keep the system observable in the case of the loss of any main PMU or the loss of a branch are to be placed at buses 1, 6, 10, and 11.

Table 3. ITS results in the case of the loss of a single branch.

Branch out	Locations of the extra PMUs
1–2	6, 10
2–3	1, 6, 10
3–4	6
4–5	6
4–8	11
5–6	6
5–8	1
6–7	6
7–9	1, 6
8–10	1, 6
9–10	1, 6
9–11	6
11–12	6
12–13	6

Table 4. The ITS results in the case of the loss of a single PMU.

Out PMU at bus	Locations of the extra PMUs
3	1, 11
7	6, 11
8	6, 10
12	1, 11

6. Out-of-step prediction algorithm

The test systems are simulated using the power system computer aided design (PSCAD) software program. The phase difference among several generators is detected from the voltage data recorded at the generator buses, and then the OOS prediction algorithm is used to predict the phase difference in advance. There are many methods to estimate and predict the dynamic variables of motors and generators [24–27].

If the predicted phase difference exceeds the instability threshold value, the system is considered to be unstable. The OOS prediction algorithm is carried out using M-file MATLAB programs.

6.1. Calculations of the predicted value for the phase difference

In [27], the authors used the phase difference values for the present time and previous time to predict the future phase difference value. This method is described using Figure 2.

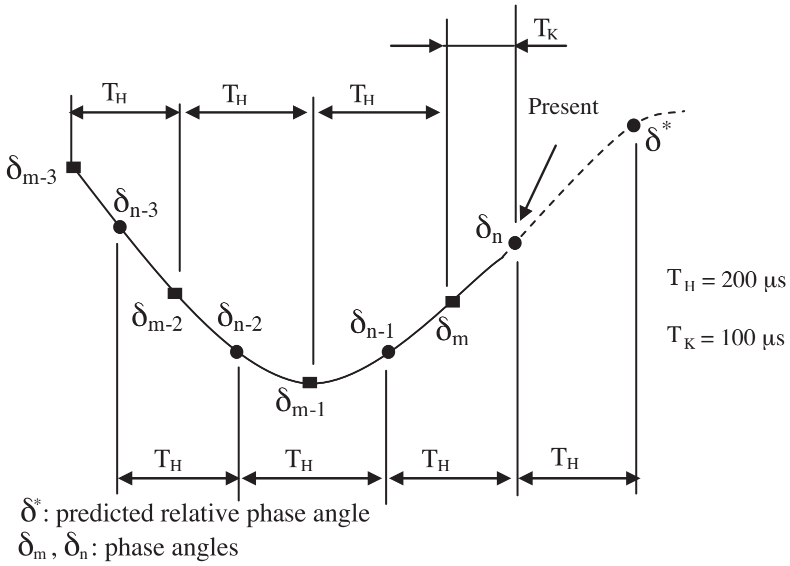

Figure 2. Method of predicting the phase difference.

The predicted phase difference δ^* for time T_H in the future is derived from the 8 pieces of data indicated in Figure 2. These are the phase differences at time T_K, before the present time, and in addition, 3 values for this time minus increments of time T_H $(\delta_m, \delta_{m-1}, \delta_{m-2}, \delta_{m-3})$ and the phase differences at the current time n, and in addition, 3 values for this time minus increments of T_H $(\delta_n, \delta_{n-1}, \delta_{n-2}, \delta_{n-3})$. Eqs. (20) through (24) are used to perform the calculation:

$$\delta^* = \delta_n + \lambda d_n + \mu d_{n-1} \tag{20}$$

where

$$d_n = \delta_n - \delta_{n-1}, d_{n-1} = \delta_{n-1} - \delta_{n-2}, d_{n-2} = \delta_{n-2} - \delta_{n-3}, \tag{21}$$

$$d_m = \delta_m - \delta_{m-1}, d_{m-1} = \delta_{m-1} - \delta_{m-2}, d_{m-2} = \delta_{m-2} - \delta_{m-3}, \tag{22}$$

$$\lambda = (d_n d_{m-2} - d_m d_{n-2})/(d_{n-1} d_{m-2} - d_{m-1} d_{n-2}), \tag{23}$$

$$\mu = (d_{n-1} d_m - d_{m-1} d_n)/(d_{n-1} d_{m-2} - d_{m-1} d_{n-2}). \tag{24}$$

Values of 200 μs and 100 μs were selected for T_H and T_K, respectively, in order to predict accurately.

6.2. Threshold value ($\delta_{\mathbf{critical}}$)

When the predicted phase difference value δ^* obtained by Eq. (20) exceeds the setting value ($\delta_{critical}$), it is judged that the generator is unstable. $\delta_{critical}$ is the threshold value used to judge the stability. The value for $\delta_{critical}$ is determined by testing the system under varying conditions. The selected value must guarantee operation when the system is unstable and must prevent operation when the system is stable [27].

7. OOS prediction test results

The previously explained prediction algorithm was applied to the phase difference between different generator buses of the test systems and the slack bus, as recorded by simulating the systems on the PSCAD software. The sampling time was 100 μs. The following are some results of the proposed algorithm.

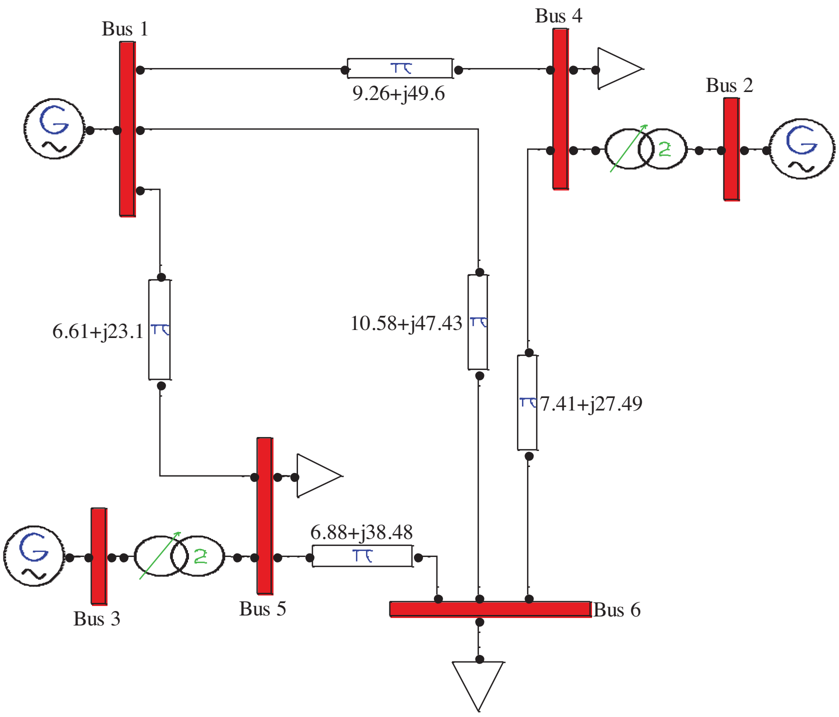

Figure 3. The model of the IEEE 6-bus system.

7.1. IEEE 6-bus system

The model of the IEEE 6-bus system is shown in Figure 3. For a 3-line-to-ground (3LG) fault at bus 4, the recorded phase difference between Gen.2 and Gen.1 (slack bus generator) is shown in Figure 4. The predicted phase difference and both the recorded and the predicted phase differences together are shown in Figures 5 and 6, respectively.

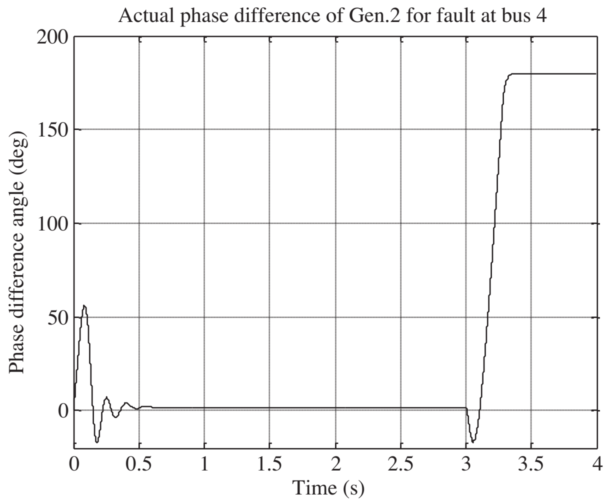

Figure 4. The recorded phase difference between Gen.2 and Gen.1 for a 3LG fault at bus 4.

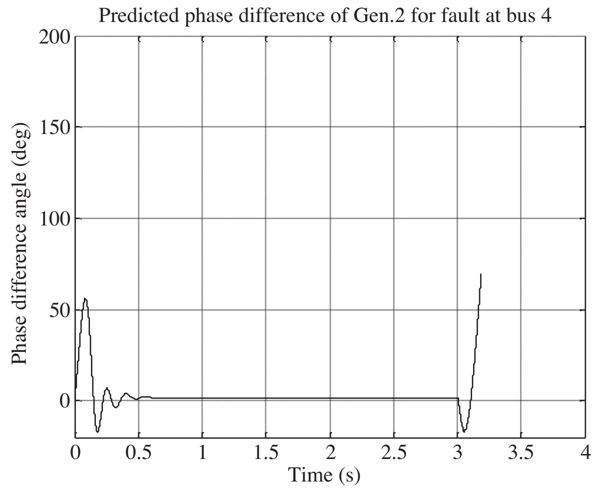

Figure 5. The predicted phase difference between Gen.2 and Gen.1 for a 3LG fault at bus 4.

As shown in Figure 6, the predicted and recorded phase difference angles are almost the same, which prove the accuracy of the prediction algorithm used.

For the same fault at bus 4, the recorded phase difference between Gen.3 and Gen.1 (slack bus generator) is shown in Figure 7. The predicted phase difference and both the recorded and the predicted phase differences together are shown in Figures 8 and 9, respectively.

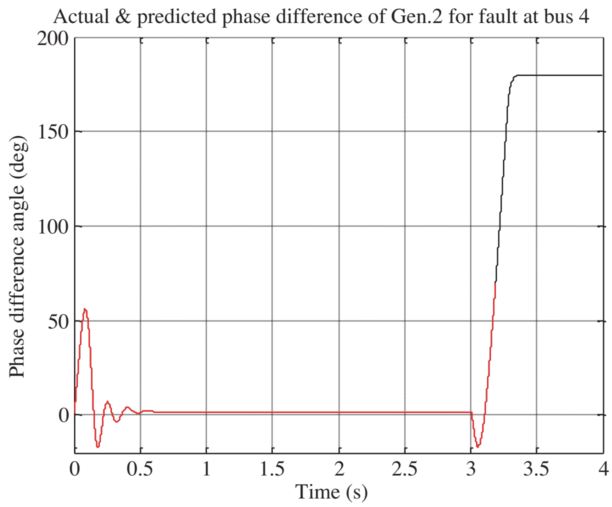

Figure 6. The recorded and predicted phase difference between Gen.2 and Gen.1 for a 3LG fault at bus 4.

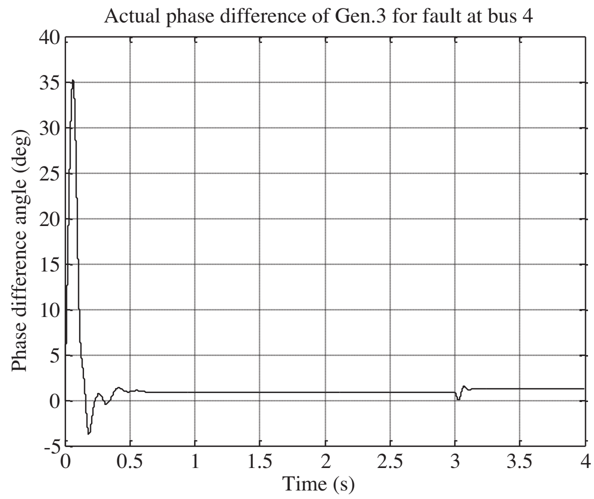

Figure 7. The recorded phase difference between Gen.3 and Gen.1 for a 3LG fault at bus 4.

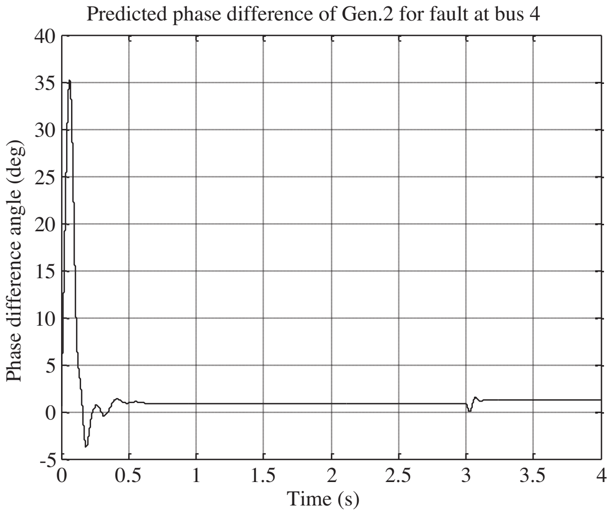

Figure 8. The predicted phase difference between Gen.3 and Gen.1 for a 3LG fault at bus 4.

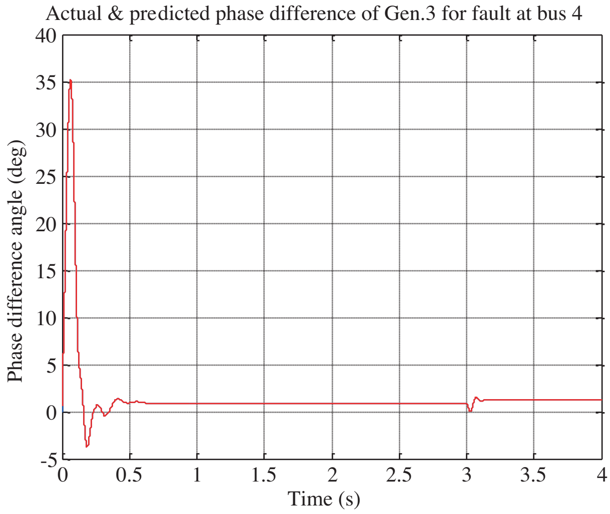

Figure 9. The recorded and predicted phase difference between Gen.3 and Gen.1 for a 3LG fault at bus 4.

As shown in Figure 9, the predicted and recorded phase difference angles are almost the same, which further prove the accuracy of the prediction algorithm used.

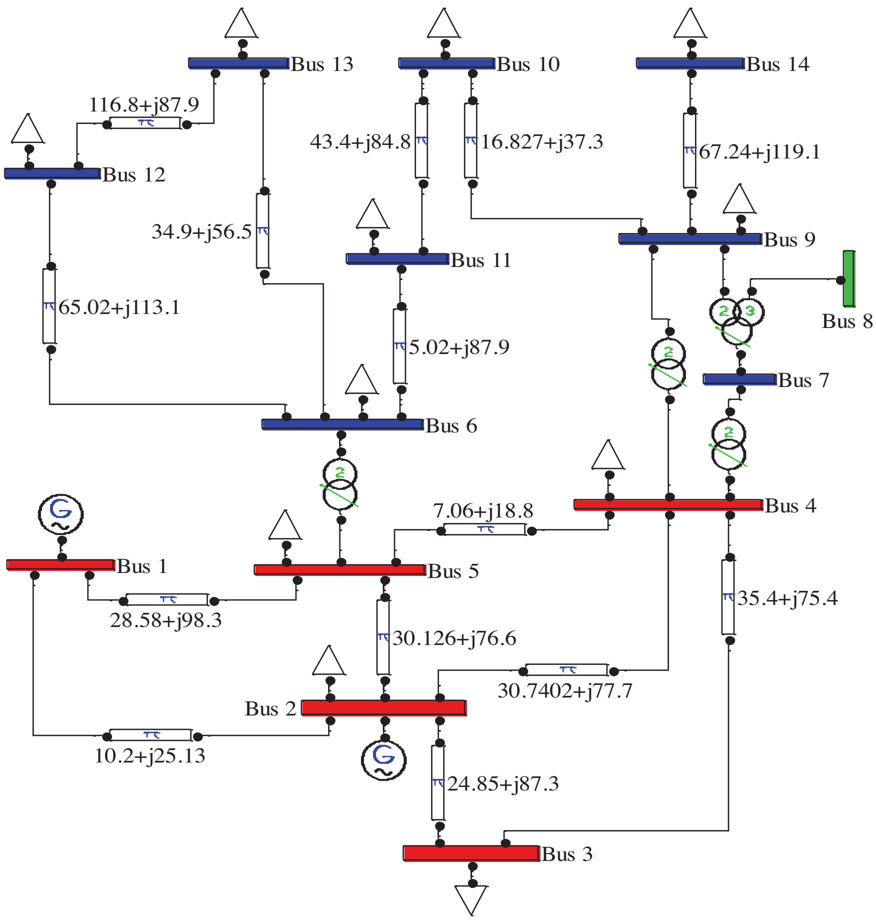

Figure 10. The model of the IEEE 14-bus system.

Through several tests of the system during faults of different types and different locations, the minimum threshold value ($\delta_{critical}$) of both generators was found to be 75°. Referring to Figures 4 and 7, under the same fault conditions, Gen.2 is out of step and Gen.3 remains stable, where the phase difference angle of Gen.2 exceeded its critical value, while that of Gen.3 did not.

7.2. IEEE 14-bus system

The model of the IEEE 14-bus system is shown in Figure 10.

For a 3LG fault at bus 2, the recorded phase difference between Gen.2 and Gen.1 (slack bus generator) is shown in Figure 11. As shown in Figure 11, Gen.2 is out of step where its phase difference angle exceeded its critical value.

The predicted phase difference and both the recorded and the predicted phase differences together are shown in Figures 12 and 13, respectively. As shown in Figure 13, the predicted and recorded phase difference angles are almost the same.

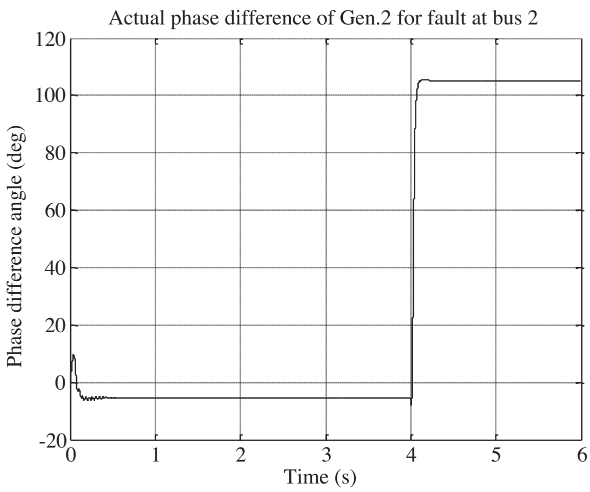

Figure 11. The recorded phase difference between Gen.2 and Gen.1 for a 3LG fault at bus 2.

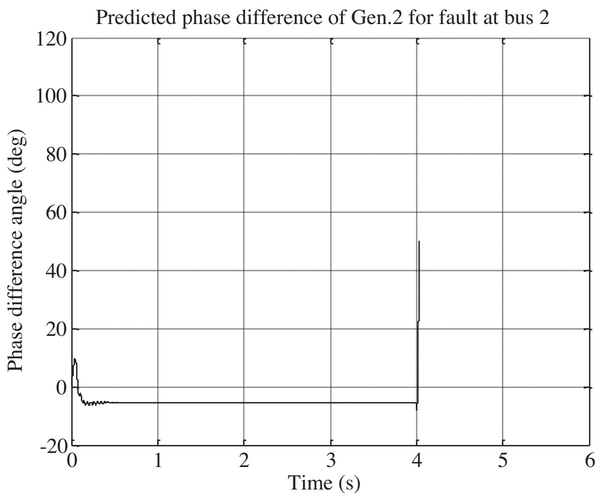

Figure 12. The predicted phase difference between Gen.2 and Gen.1 for a 3LG fault at bus 2.

Through several tests of the system during faults of different types and different locations, the minimum threshold value ($\delta_{critical}$) of generator 2 was found to be 60°. As shown in Figure 10, under a 3LG fault at bus 2, Gen.2 is out of step where its phase difference angle exceeded its critical value.

7.3. Egyptian 500 kV network

The model of the Egyptian 500 kV network is shown in Figure 14.

As a sample of the test results, the phase difference angles at Gen.3 during the 3LG fault at bus 7 are presented. For a 3LG fault at bus 7, the recorded phase difference between Gen.3 and Gen.1 (slack bus generator) is shown in Figure 15. The predicted phase difference and both the recorded and the predicted phase differences together are shown in Figures 16 and 17, respectively.

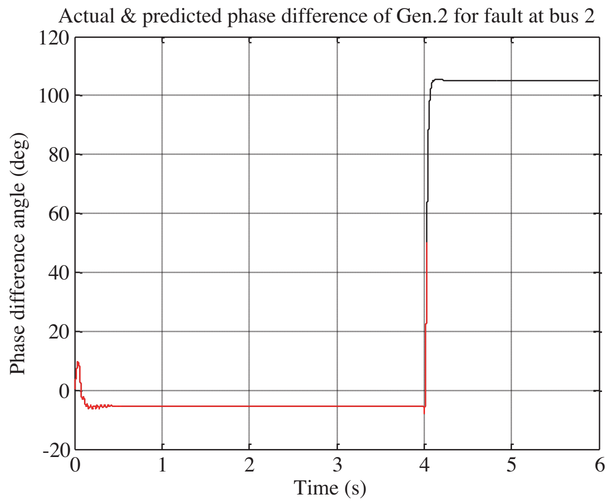

Figure 13. The recorded and predicted phase difference between Gen.2 and Gen.1 for a 3LG fault at bus 2.

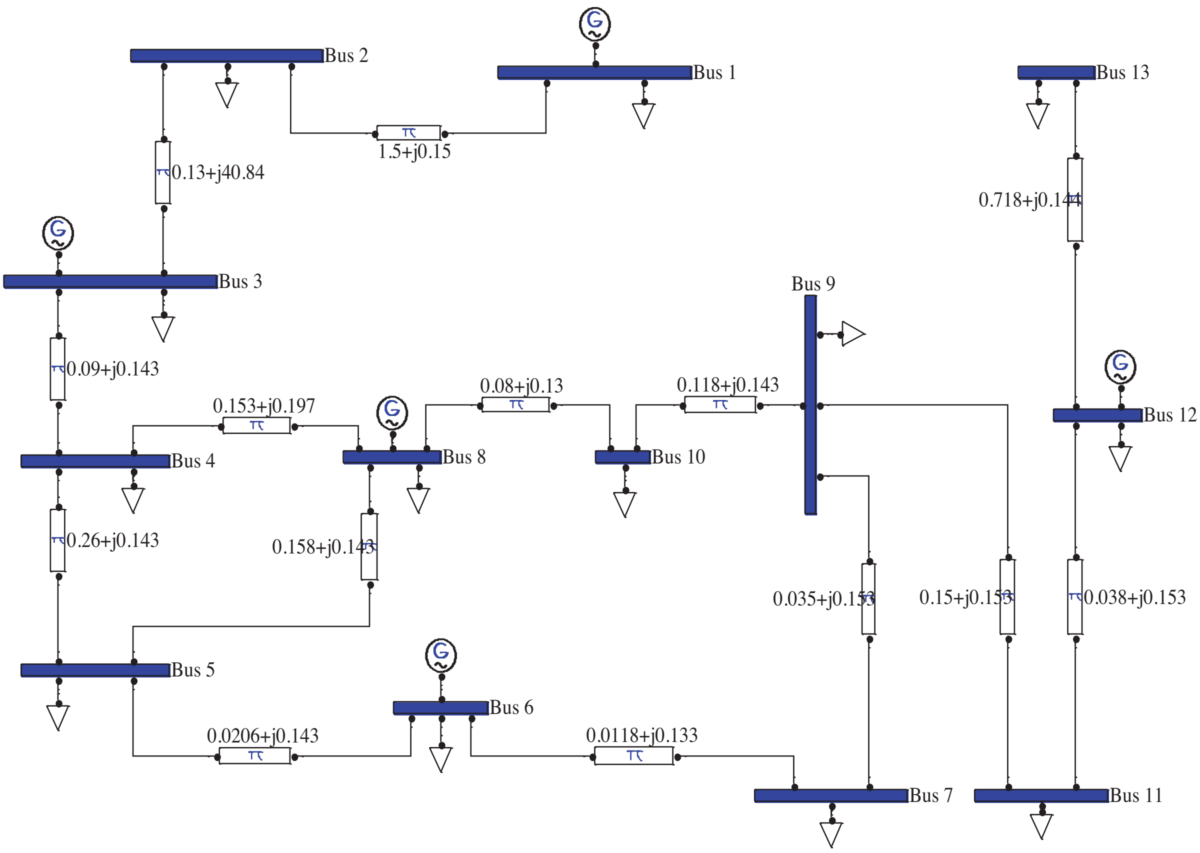

Figure 14. The PSCAD model of the Egyptian 500 kV network.

Through several tests of the system during faults of different types and different locations, the minimum threshold value (δ critical) of all of the generators was found to be 50°. As shown in Figure 15, for a 3LG fault at bus 7, Gen.3 is out of step where its phase difference angle exceeded the critical value.

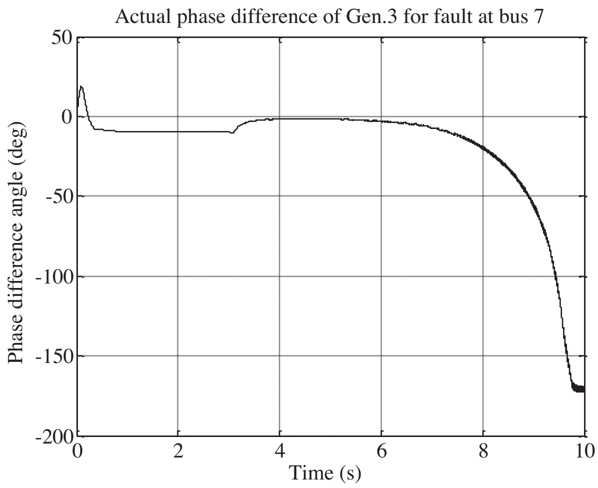

Figure 15. The recorded phase difference between Gen.3 and Gen.1 for a 3LG fault at bus 7.

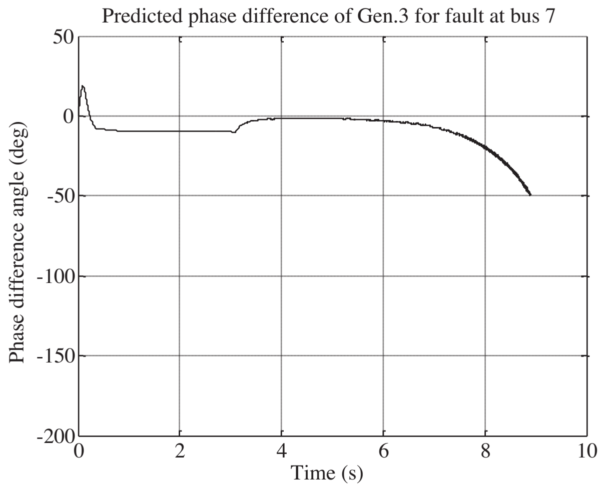

Figure 16. The predicted phase difference between Gen.3 and Gen.1 for a 3LG fault at bus 7.

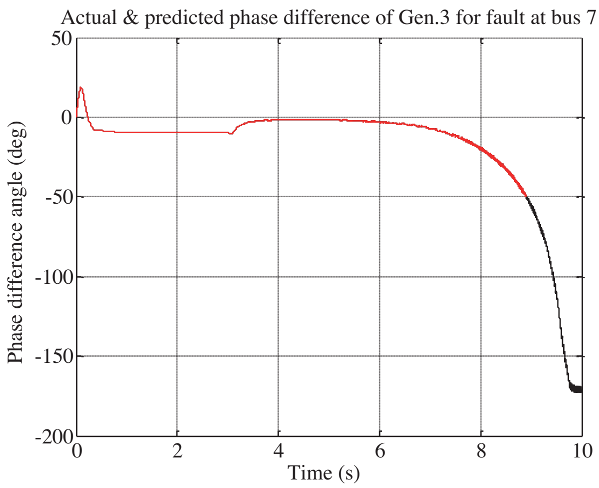

Figure 17. The recorded and predicted phase difference between Gen.3 and Gen.1 for a 3LG fault at bus 7.

8. Conclusion

This paper proposed an optimization method for the optimal placement of PMUs for the complete observability of power systems. The proposed method is based on numerical observations and artificial intelligence. The artificial intelligence algorithm used is the ITS algorithm, which is used to find the optimal placement for the PMU to keep the system completely observable. The proposed algorithm is also applied to find the additional PMU to be placed to keep the system observable in the case of the loss of a single PMU or a single branch. This way, a set of PMUs is found to keep the system completely observable under normal and contingency conditions. The results were consistent with previously reported results. In addition, the paper described a predictive OOS algorithm based on the observation of the voltage phase difference between the substations. The proposed optimal placement of the PMUs and the OOS algorithms was tested using the IEEE 6-bus and IEEE 14-bus systems, and the Egyptian 500 kV network. The test systems were simulated using the PSCAD software. The placement algorithm and the OOS prediction algorithm were carried out using MATLAB script programs. The test results showed the effectiveness of both the PMU's placement and the prediction algorithms introduced.

References

[1] A.G. Phadke, "Synchronized phasor measurements in power systems", IEEE Computer Applications in Power, Vol. 6, pp. 10–15, 1993.

[2] T.L. Baldwin, L. Mili, M.B. Boisen, R. Adapa, "Power system observability with minimal phasor measurement placement", IEEE Transactions on Power Systems, Vol. 8, pp. 707–715, 1993.

[3] R.F. Nuqui, A.G. Phadke, "Phasor measurement unit placement techniques for complete and incomplete observability", IEEE Transactions on Power Delivery, Vol. 20, pp. 2381–2388, 2005.

[4] B. Milosevic, M. Begovic, "Nondominated sorting genetic algorithm for optimal phasor measurement placement", IEEE Transactions on Power Systems, Vol. 18, pp. 69–75, 2003.

[5] B. Xu, A. Abur, Optimal placement of phasor measurement units for state estimation, Final Project Report, Power Systems Engineering Research Center, 2005.

[6] B. Xu, A. Abur, "Observability analysis and measurement placement for systems with PMUs", Proceedings of the IEEE PES Power Systems Conference and Exposition, Vol. 2, pp. 943–946, 2004.

[7] C. Rakpenthai, S. Premrudeepreechacharn, S. Uatrongjit, N.R. Watson, "An optimal PMU placement method against measurement loss and branch outage", IEEE Transactions on Power Delivery, Vol. 22, pp. 101–107, 2005.

[8] J. Peng, Y. Sun, H.F. Wang, "Optimal PMU placement for full network observability using Tabu search algorithm", Electrical Power and Energy Systems, Vol. 28, pp. 223–231, 2006.

[9] A. Sadu , R. Kumar, R.G. Kavasseri , "Optimal placement of phasor measurement units using particle swarm", Proceedings of the World Congress on Nature and Biologically Inspired Computing, pp. 1708 –1713, 2009.

[10] S. Chakrabarti, E. Kyriakides, "Optimal placement of phasor measurement units for power system observability", IEEE Transactions on Power Systems, Vol. 23, pp. 1433–1440, 2008.

[11] C. Rakpenthai, S. Premrudeepreechacharn, S. Uatrongjit, N.R. Watson, "An optimal PMU placement method against measurement loss and branch outage", IEEE Transactions on Power Delivery, Vol. 22, pp. 101–107, 2007.

[12] M. Hurtgen, J.C. Maun, "Optimal PMU placement using iterated local search", Electrical Power and Energy Systems, Vol. 32, pp. 857–860, 2010.

[13] A. Ahmadi, Y. Alinejad-Beromi, M. Moradi, "Optimal PMU placement for power system observability using binary particle swarm optimization and considering measurement redundancy", Expert Systems with Applications, Vol. 38, pp. 7263–7269, 2011.

[14] M. Hajian, A. M. Ranjbar, T. Amraee, B. Mozafari, "Optimal placement of PMUs to maintain network observability using a modified BPSO algorithm", Electrical Power and Energy Systems, Vol. 33, pp. 28–34, 2011.

[15] K. Jamuna, K.S. Swarup, "Optimal placement of PMU and SCADA measurements for security constrained state estimation", Electrical Power and Energy Systems, Vol. 33, pp. 1658–1665, 2011.

[16] S.H. Horowitz, A.G. Phadke, Power System Relaying, New York, Wiley, 1995.

[17] C.W. Taylor, J.M. Haner, L.A. Hill, W.A. Mittelstadt, R.L. Cresap, "A new OS relay with rate of change of apparent resistance augmentation", IEEE Transactions on Power Systems, Vol. PAS-102, pp. 631–639, 1983.

[18] W.R. Roemish, E.T. Wall, "A new synchronous generator out-of-step relay scheme, Part I: abbreviated version", IEEE Transactions on Power Systems, Vol. PAS-104, pp. 563–571, 1985.

[19] T.L. Baldwin, L. Mili, M.B. Boisen Jr, R. Adapa, "Power system observability with minimal phasor measurement placement", IEEE Transactions on Power Systems, Vol. 8, pp. 707–715, 1993.

[20] B. Gou, A. Abur, "A direct numerical method for observability analysis", IEEE Transactions on Power Systems, Vol. 15, pp. 625–630, 2000.

[21] F. Glover, "Tabu search: Part I", ORSA Journal on Computing, Vol. 1, pp. 190–206, 1989.

[22] F. Glover, "Tabu search: Part II", ORSA Journal on Computing, Vol. 2, pp. 4–32, 1990.

[23] W.M. Lin, F.S. Cheng, M.T. Tsay, "An improved tabu search for economic dispatch with multiple minima", IEEE Transactions on Power Systems, Vol. 17, pp. 108–112, 2002.

[24] S. Aksoy, A. Mühürcü, "Elman neural network-based nonlinear state estimation for induction motors", Turkish Journal of Electrical Engineering & Computer Sciences, Vol. 19, pp. 861–875, 2011.

[25] M.G. Aydeniz, İ. Şenol, "A Luenberger-sliding mode observer with rotor time constant parameter estimation in induction motor drives", Turkish Journal of Electrical Engineering & Computer Sciences, Vol. 19, pp. 901–912, 2011.

[26] I. Shoukry, E.D. Kunt, A. Sabanovic, "Action-reaction based parameters identification and states estimation of flexible systems", Turkish Journal of Electrical Engineering & Computer Sciences, Vol. 20, pp. 47–56, 2012.

[27] M. Suzuki, K. Yanagihashi, M. Yamaura, K. Omata, T. Nakamura, S. Mitamura, H. Watanabe, "A predictive out-of-step protection system based on observation of the phase difference between substations", IEEE Transactions on Power Delivery, Vol. 5, pp. 1695–1704, 1990.